Early brain changes in Lyme disease are associated with clinical outcomes

Cherie L. Marvel[1,2], Alison W. Rebman[3], Kylie H. Alm[2], Pegah Touradji[4], Arnold Bakker[1,2], Prianca A. Nadkarni[1], Deeya Bhattacharya[1], Owen P. Morgan[1], Amy Mistri[1], Christopher Sandino[1], Jonathan Ecker[1], Erica A. Kozero[3], Arun Venkatesan[1], Abhay Moghekar[1], Ashar Keeys[1], and John N. Aucott[3]

Abstract

Lyme disease (LD) is a tick-borne infection due to the bacteria *Borrelia burgdorferi*. After antibiotic treatment, 10-20% of patients develop post-treatment Lyme disease (PTLD). Neurological symptoms are commonly reported in PTLD. This case-control study tested the hypothesis that brain changes occur in LD and are related to clinical outcomes.

A working memory task was administered during functional MRI (fMRI), in conjunction with cognitive assessments and health surveys, to examine brain function and clinical outcomes in people with acute LD disease (n=20; 55.0% male; mean age (range) = 52.3 (26-78)). Assessments were conducted a mean of 15.2 days (range: 1-51) after initial antibiotic treatment [i.e., “baseline”] and again 6 months later. A well-matched group of healthy controls (HC, n=19; 31.6% male; mean age (range) = 46.5 (19-60)) was also assessed 6 months apart. At the 6-month follow-up, the LD group was categorized into those who returned to health (RTH, n=11) and those reporting persistent symptoms (sPTLD, n=9) to determine if early brain changes predicted subsequent outcomes. FMRI data from both LD groups were compared to the HC group. Regions of interest (ROI) values were obtained from the fMRI results and correlated to cognitive performance and symptom survey scores.

At baseline, brain activity in the RTH group was significantly increased relative to that of HC. Notably, 64% of the RTH group’s activation clusters were in white matter, confirmed by segmentation analysis. ROIs created from the RTH vs. HC fMRI results, including white matter regions, significantly correlated with better self-reported clinical outcomes. At the 6-month follow-up, most of the RTH group’s activity had normalized relative to HC, and associations between ROI values and clinical outcomes were no longer observed. The sPTLD group showed few fMRI activation differences versus the HC group at either time point, and

no significant associations were observed between ROI values and clinical outcomes. Instead, the sPTLD group's ROI values negatively correlated with cognitive performance at the 6-month follow-up.

These results indicate that early brain changes in LD predict future RTH status. Increased brain activation during cognition, including in white matter, may reflect a healing response without which LD patients are more likely to develop PTLD. The observed increased activation in white matter suggests specific mechanisms, such as appropriate astrocyte reactivity, and require further investigation. Understanding how increased brain activity relates to RTH in LD will aid early identification of those vulnerable to developing PTLD and guide treatment.

[1]Department of Neurology, Johns Hopkins University School of Medicine, Baltimore, MD, 21205, United States of America

[2]Department of Psychiatry and Behavioral Sciences, Johns Hopkins University School of Medicine, Baltimore, MD, 21205, United States of America

[3]Division of Rheumatology, Department of Medicine, Lyme Disease Research Center, Johns Hopkins University School of Medicine, Baltimore, MD, 21205, United States of America

[4]Deparment of Physical Medicine and Rehabilitation, Johns Hopkins University School of Medicine, Baltimore, MD, 21205, United States of America

Correspondence to: Cherie L. Marvel

1501 E. Jefferson Street, Baltimore, MD 21287, USA

Cmarvel1@jhmi.edu

Running title: Brain changes in Lyme disease

Keywords: MRI; PTLD; tickborne; cognition; white matter; astrocyte

Introduction

Lyme disease (LD) is an inflammatory disease initiated by infection with *Borrelia burgdorferi* (Bb) following the bite of an infected tick. Signs of untreated infection range from the erythema migrans rash during early disease to later systemic disease that can involve the central and peripheral nervous systems, as well as the cardiac and musculoskeletal systems.[1] After standard of care antibiotic therapy, 10-20% of patients treated for LD will develop a chronic syndrome of patient-reported symptoms, known as post-treatment Lyme disease (PTLD).[2,3] The Infectious Disease Society of America (IDSA)-proposed case definition of PTLD includes prior physician-documented LD, appropriate antibiotic treatment, and development of subjective complaints of fatigue, widespread musculoskeletal pain, and/or cognitive difficulties within six months of the LD diagnosis that lasts for at least six months, and results in significant social or functional decline.[4-6] Little is known about the pathophysiology of or risk factors for PTLD, and there are no FDA-approved therapeutics for curative treatment. Importantly, clinicians currently cannot identify patients who are at risk of developing PTLD at the time of acute infection.[7]

Patient-reported cognitive symptoms are common among patients with PTLD.[8] One study reported significant cognitive decline in 25% of a cohort of patients with PTLD.[9] Another 25% were excluded due to sub-optimal effort, which may have represented an indicator of dysfunction in its own right. A startling 92% of the entire cohort with PTLD complained of cognitive difficulties. Of those who met definition for cognitive decline, the affected processes involved visual search speed, information processing speed, mental flexibility, attention, working memory, executive functioning, and verbal memory. Due to its high prevalence, neurocognitive dysfunction could be a key phenotype in the pathophysiology and impact of PTLD. However, cognitive impairments can be associated with other illness-related factors, such as sleep disturbance, mood difficulties, fatigue, pain, and poor health-related quality of life, all of which can be significant in those with PTLD.[6] Teasing apart the contributions of these individual factors to cognition in PTLD, and their relationship to underlying pathology, can be challenging.[6,10,11]

To date, only a handful of investigations have conducted *in vivo* brain studies of LD patients. One study observed increased glial cell activity throughout the brain,[12] suggesting that neuronal health had been compromised and required glial support. In a separate study, generalized decreased cerebral blood flow was noted, though several increases were observed

within white matter.[13,14] In a recent study, PTLD and healthy control participants performed a working memory task while undergoing functional MRI (fMRI).[15] In the PTLD group relative to controls, white matter activations were observed, a phenomenon which has been described but is highly unusual.[16-18] The white matter fMRI-guided regions of interest (ROI) were examined further using diffusion MRI methods to assess white matter tract integrity. Interestingly, higher axial diffusivity (AD) within these ROIs was associated with *fewer* cognitive and neurological symptoms. Results from these studies show that the brain can be altered during PTLD, and that these alterations tend to involve white matter, and, paradoxically, that the white matter changes observed may be associated with better clinical outcomes. It is not known whether these white matter changes emerge prior to the clinical presentation of PTLD and if so, if they also predict better clinical outcomes.

The current case-control longitudinal study examined brain changes associated with early LD within weeks of the first diagnosis of erythema migrans and acute infection and again 6 months later. We hypothesized that white matter changes would emerge early (within 6 months after infection), which is the duration that meets the IDSA-proposed definition of PTLD criteria. We also hypothesized that white matter changes would be associated with better clinical outcomes, consistent with the prior findings in a cross-sectional PTLD cohort.[15]

Materials and methods

Participants

The Institutional Review Board of the Johns Hopkins University School of Medicine approved this study. Written informed consent was obtained between 2017-2022 according to the Declaration of Helsinki from all participants prior to initiation of study activities, and all participants received compensation.

A total of 23 adults with early LD consented for this study. They were recruited from the Johns Hopkins Lyme Disease Research Center in which they were enrolled in the on-going Study of Lyme Immunology and Clinical Events (SLICE).[19] At the time of SLICE study enrollment, participants were required to have a visible, diagnostic erythema migrans rash $\geq$ 5 cm and to not have been ill longer than 3 months. Patients were excluded if they self-reported a medical history of any conditions with significant symptom overlap with PTLD, similar to

those listed in the IDSA's proposed case definition.[4] Specifically, those with fibromyalgia, chronic fatigue, major immunosuppression, psychiatric or autoimmune illnesses, hepatitis B/C, HIV, cancer chemotherapy treatment in the past two years, a history of illicit drug or substance abuse, Long COVID, or current pregnancy were excluded. In the current study, participants were seen for their baseline fMRI visit after completing three weeks of doxycycline treatment, an average of 42.3 days after the onset of their LD.

A total of 21 adults consented for this study as healthy control participants (HC group). They were recruited via community flyers and screened for any co-morbid conditions with significant symptom overlap with PTLD, as well as the exclusion criteria described above, or a past diagnosis of LD.

In a final screening stage, both LD and HC participants were excluded from study participation if they endorsed the following characteristics that might confound data interpretation: history of major neurologic disorders (including history of stroke, seizures, or HIV); a prior head injury resulting in loss of consciousness for greater than 5 minutes; current severe or unstable medical disorder; history before LD of a significant learning disability; and history before LD of a severe mood or psychotic disorder. Participants were also excluded contraindications within the MRI environment, such as metal or surgical implants and claustrophobia. Finally, participants were excluded for left-handedness or being a non-native English speaker (unless English was learned before puberty) because each of these would confound results due to the nature of the verbal working memory task administered in during fMRI. (Table 1)

Participants were asked to return six months after their MRI to re-assess clinical and cognitive variables, obtain a second MRI, and determine health outcomes post infection. Data were removed from analyses if a participant dropped out of the SLICE study before an outcome could be ascertained, fMRI data was unusable, or there was an incidental MRI finding. In some cases, participants did not return for their follow-up MRI, but remained in the SLICE study, enabling a health outcome determination, and their baseline data were included. This resulted in a final sample of 20 LD participants included in the baseline and 17 in the follow-up analysis, and 19 HC participants included in the baseline and 16 in the follow-up analysis (Fig. 1).

Clinical assessment

Overall health, mood, symptom severity, fatigue, pain and health-related quality of life were assessed by standardized questionnaires which were administered at the baseline and 6-month visits. The Short Form Health Survey, version 2 (SF-36)[20] is a 36-item measure of functioning in eight health attributes: Physical Functioning, Role of Physical (on daily living), Bodily Pain, General Health, Vitality, Social Functioning, Role of Emotional (on daily living), and Mental Health. These scores can also be compared to the US population mean (50.0 ± 10.0). The Fatigue Severity Scale (FSS)[21] is a 9-item measure of the impact of fatigue on daily function, with scores ranging from 9 to 63. Pain was measured by the Short-Form McGill Pain Questionnaire-2 (SF-MPQ-2),[22] a 15-item pain metric with total summary scores ranging from 0 to 45. The Beck Depression Inventory II (BDI-II)[23] is a 21-item depression metric with summary scores ranging from 0 to 63 with the following clinical classifications: 0-13, minimal depression; 14-19, mild depression; 20-28, moderate depression, and 29-63, severe depression. Cognitive-Affective (BDI-CA) and Somatic (BDI-S) factor scores were also calculated. Additionally, participants self-administered a 36-item measure of symptom presence and severity (the post-Lyme Questionnaire of Symptoms [PLQS]) developed from prior clinical and research experience among patients with PTLD.[24] For all questionnaires, higher scores indicate more severe symptoms, except on the SF-36 where higher scores indicate higher health-related quality of life and functioning.

Patient outcome status (return to heath [RTH] vs. symptoms of PTLD [sPTLD]) was determined at the 6-month follow-up visit. Groups were defined based on a previously published operationalized definition.[24,25] Patients met criteria for RTH if: a) their PLQS did not indicate the presence of either fatigue, musculoskeletal pain, or cognitive complaints at the ‘moderate’ or ‘severe’ level and b) if their average composite score of 4 specific norm-based subscales on the SF-36 was more than 0.5 SD below the population mean.[25] Remaining patients were considered sPTLD with either symptoms and/or functional impact present.

Cognitive assessment

Standardized cognitive tests with well-established norms were administered at each timepoint. Pre-morbid intellectual functioning was measured using the reading subtest of the Wide Range Achievement Test – 4th Edition (WRAT-4).[26] The Digit Span (DS) Subtest of the Wechsler Adult Intelligence Scale – 4th Edition (WAIS-IV)[27] was used to measure attention (DS Forward) and working memory (DS Backward and DS Sequencing). The

Hopkins Verbal Learning Test – Revised (HVLT-R)[28] was used to measure verbal learning, delayed recall and retention, and recognition memory for a verbal list-learning task. Processing speed was measured using the Trail Making Test (Trails A and Trails B)[29] and WAIS-IV Digit Symbol Coding.[27] All measures of processing speed involved visual scanning, attention, and psychomotor processing, while Digit Symbol Coding also involved working memory, and Trails B involved executive function. The Controlled Oral Word Association Test (COWA)[30] was used to assess verbal fluency, using letter and semantic cues under time constraints. All raw scores were converted to T-scores using established standardized norms.

MRI procedures

Behavioral task

Verbal working memory

Participants were asked to perform a verbal working memory task in the MRI scanner that has been described previously.[15,31,32] The paradigm involved two task conditions, each consisting of two stimulus conditions, resulting in four overall study conditions. Briefly, in the "control" condition, participants visually encoded one or two letters, and after a 4-6 second delay, they indicated by button press whether a probe letter matched a target letter. In the "forward" condition, participants again visually encoded one or two letters. During the delay period, however, they counted two alphabetical letters forward of each letter and held those new letters in mind. For example, if the letters were ''f" and ''q", participants would hold ''h" and ''s" in mind. When the probe letter appeared, participants indicated whether the probe matched the newly derived target letters. Thus, there were four conditions total: 1) one-letter control, 2) two-letters control, 3) one-letter forward, and 4) two-letters forward.

Participants were given up to 6 seconds to respond by button press (match = right index finger; non-match = right middle finger). Trials were jittered with an inter-trial interval (ITI) of 6-9 seconds. Response time (RT) and accuracy were recorded for each trial. Each participant completed one block each of the control and forward conditions, in separate scanner runs, with the order counterbalanced across participants. Each block contained 64 trials (~ 16 minutes). Probe letters matched a target (or newly derived target) on 50% of the trials. The parameters were pseudorandomized such that identical presentation occurred in no more than three consecutive trials: number of target letters (one or two), rehearsal duration (4 or 6 seconds), expected response (match or non-match), and duration of ITI (6–9 seconds).

The measures of interest were accuracy and response time for each condition, with no minimal performance threshold for data inclusion. Due to a technical error, responses from one control participant were not recorded. This participant was not included in the behavioral analysis but remained in the fMRI analysis by including all trials.

Hemodynamic response function (HRF)

Individualized HRFs were obtained for convolutions during the event-related fMRI analyses to account for potential HRF differences across participants or study groups. This was obtained via a tapping task involving the right index finger. Tapping blocks lasted ~30 seconds upon presentation of "tap" instructions, followed by "rest", also lasting ~ 30 seconds, for a total duration of 10 minutes.[15,33-35]

Equipment

Stimuli were delivered using E-Prime 2.0 software (Psychology Software Tools, Pittsburgh, PA) on a Dell Inspiron 7472 laptop running Windows 10 Pro. Participants viewed stimuli via an Epson PowerLite 7600p projected that projected onto a screen in the MRI scanner bore, which was then reflected onto a mirror attached to the top of the head coil and inclined at 45°. Due to an equipment upgrade, one Lyme participant at baseline and three Lyme participants at the 6-month follow-up visit viewed stimuli via a Cambridge Research Systems BOLDscreen 32 UHD LCD display, which was run through a mirror box, then projected onto the head coil-mounted mirror. Button-press responses were collected using two fiber optic button boxes (MRA, Inc., Washington, PA) held by the participant in their right hand during the tasks.

MRI data acquisition

All MRI data were acquired on a Philips 3 Tesla scanner using a 32-channel head coil.

Structural MRI

A sagittal magnetization prepared gradient-echo (MPRAGE) sequence aligned to the anterior-posterior commissure (AC-PC) axis was used with the following parameters: repetition time (TR)/echo time (TE) = 7/3.3 ms; field of view = 240 mm x 240 mm; 170 slices; slice thickness 1.0 mm; 0 mm gap; flip angle = 8 degrees; voxel size = 0.75 mm x 0.75 mm. The total scan duration was 6 minutes.

Functional MRI

A T2-weighted gradient echo EPI pulse sequence was used with the following parameters: TR = 1000 ms; TE = 30 ms; flip angle = 61 degrees; in-plane resolution = 3.75 mm; slice thickness = 6 mm with a 1 mm gap; 20 oblique-axial slices; FOV = 21mm x 240 mm. To maximize whole-brain coverage to include the cerebellum and neocortex, images were acquired in the oblique-axial plane rotated 25 degrees clockwise with respect to the AC-PC line. The number of acquired volumes within each run ranged from 917 to 922 for the working memory tasks and 630 for the tapping task. The start of the fMRI scan was triggered by Eprime 2.0 software (Psychology Software Tools, Pittsburgh, PA) at the beginning of each run.

MRI data analysis

Functional data analysis

Standard image preprocessing steps were performed using SPM12 (http://fil.ion.ucl.ac.uk/spm/): slice timing correction (reference = slice #10), motion correction, anatomical co-registration, normalization to the Montreal Neurological Institute (MNI) stereotaxic space, and spatial smoothing (FWHM = 8 mm). Individual HRF regressors were convolved with reference waveforms for the delay phase of the task (i.e., the 4-6 second delay between target and probe presentation) for each subject within the first-level analysis. This represented an event-related analysis focusing on working memory in the absence of visual stimuli or motor response. Statistical maps were computed for each subject using the general linear model approach with high pass filtering of 128 seconds. A random effects analysis was performed to map the average responses for correct trials only. All trials were included for one control at baseline whose behavioral data was not recorded due to a technical error. A beta contrast volume per subject was computed and used to conduct one-sample t-test values at every voxel. Within-group contrasts compared the blood oxygen level dependence (BOLD) signal difference between the two-letters forward minus two-letters control conditions. These differences were compared between group pairs (i.e., All Lyme vs. HC, RTH vs. HC, sPTLD vs. HC, and RTH vs. sPTLD). Activations were identified using a threshold of $p < .001$ with a cluster-level $k \geq 10$. ROIs were created from surviving clusters using the Mars-BaR toolbox for SPM.[36] Individual ROI values were segmented for tissue classification. ROIs containing > 50% white matter were considered white matter activations. Gray and white matter activations were correlated with cognitive and clinical variables. For

anatomical determinations of the activations, MNI coordinates were transformed into the coordinate system of the Talairach and Tourneaux stereotaxic atlas[37] using Bioimage Suite Web (Version 1.2.0, https://bioimagesuiteweb.github.io/webapp/mni2tal.html) and cross-referenced with atlas manuals.[37,38]

Tissue class segmentation analysis

Following methods developed previously,[15] significant clusters of fMRI activation for each contrast and timepoint of interest were first transformed into binary ROIs masks, and then resampled into 1 mm^3 space using nearest neighbor interpolation to match the MPRAGE template space used for tissue class segmentation. A study-specific T1 modal model template was generated for the segmentation analysis using all participants and all timepoints. Advanced Normalization Tools (ANTs) software[39,40] was used to calculate a 3D vector field transformation for each MPRAGE image input aligned to a template modal model generated from the entire sample. FSL's FAST automated segmentation[41,42] was used to segment the template MPRAGE image into three tissue classes: gray matter, white matter, and cerebrospinal fluid. Each binary ROI mask was multiplied by the binary white matter segmentation mask generated by FAST, which yielded the number of white matter voxels within each ROI. This value was divided by the number of voxels in the entire ROI and multiplied by 100 to yield the percentage of white matter voxels. ROIs that contained > 50% white matter were categorized as "white matter activations" in subsequent analyses.

ROI analysis with clinical & cognitive variables

The estimate of activation within gray and white matter clusters were computed using MarsBar.[36] All voxel values within the ROI were averaged to yield one value per ROI. This value was correlated to variables obtained from questionnaires and cognitive tests.

Statistical analysis

The clinical, cognitive, and MRI data collected in this study contained continuous variables, except gender, which was categorical. In group comparisons (RTH vs. sPTLD, RTH vs. controls, and sPTLD vs. controls), t-tests and one-way ANOVA tests were used to compare continuous variables (e.g., age and education), and Fisher's Exact test was used to compare gender. P-values for t-tests were determined by the result of the Levene's Test for Equality of Variances. Shapiro-Wilk tests were used to determine if continuous variables followed a normal distribution. If a variable was not normally distributed, Mann-Whitney U-tests and

Kruskal-Wallis tests were conducted to compare groups. Mixed-design ANOVAs were used to compare repeated measures between groups (e.g., fMRI task performance). [No ANOVAs contained a within-subjects factor with more than two levels; sphericity corrections were, therefore, not needed.] If the mixed-design ANOVAs revealed group effects, pairwise t-tests were conducted to determine which groups were affected differentially. When controlling for specific variables, ANCOVAs (with univariate ANOVAs) were used to compare groups in place of t-tests for normally distributed variables. For non-parametric variables, the ANCOVAs were performed after the dependent and covaried variables had been rank-transformed. Pearson correlations were used when the Shapiro-Wilk's normality tests indicated a normal data distribution (e.g., correlating ROI values with symptom measures). Otherwise, Spearman's rho nonparametric correlations were used for variables with non-normal data distributions or as noted. Missing data within a symptom rating scale was imputed such that the mean for all other symptom items for an individual was entered as the missing value and fed into the summary score. All tests were two-tailed, with an alpha level < .05 to define statistical significance. Statistics were performed using IBM SPSS Statistics, Macintosh, version 29 (IBM Corp., Armonk, NY, USA).

Data availability

The data that support the findings of this study are available from the corresponding author, upon reasonable request.

Results

Participants

Based on clinical and health measures obtained at 6 months, 11 Lyme participants were assigned to the RTH group and nine to the sPTLD group. (Table 1) Groups (sPTLD, RTH, and HC) did not differ by age *(H(2) = 3.02, p = .221*), years of education (*F*(2,36) = *.042, p = .959*), or gender, *p = .24*. Comparisons between the RTH and sPTLD groups revealed no differences in the median days' duration between LD onset and receiving antibiotic treatment (RTH = 4.00 vs. sPTLD = 6.00, *U = 46.0, p = .819),* between LD onset and receiving the first MRI scan (RTH = 36.00 vs. sPTLD = 38.00, *U = 56.5, p = .603*), or between ending antibiotics and receiving the first MRI scan (RTH = 10.00 vs. sPTLD = 12.00, *U = 56.5, p = .603*). Groups did not differ in the duration between MRI scans (*H(2) = .530, p = .767).*

Clinical assessment

Health survey results were analyzed between the RTH and sPTLD groups to identify differences in symptom severity at each timepoint. At baseline, the patient groups differed on the SF-36 (Social Functioning Scale, $U = 18.00$, $p = .033$; Mental Component Scale, $t(17) = 2.86$, $p = .011$) and the PLQS (Symptoms Total, $U = 68.50$, $p = .041$). At follow-up, patient groups differed on the BDI Total, $U = 11.00$, $p = .023$; the BDI Cognitive/Affective Subscale, $U = 13.00$, $p = .039$, and the PLQS (Symptoms Total, $U = 8.00$, $p = .003$). (Table 2)

Cognitive assessment

At baseline, the HC group scored significantly higher than the RTH and sPTLD groups on Trails A, (vs. RTH: $t(28) = 2.17$, $p = .038$; vs. sPTLD: $t(26) = 2.49$, $p = .019$). At follow-up, HC and patient groups showed no significant differences. The RTH vs. sPTLD groups showed no significant differences at either timepoint.

Tests were run to identify changes in cognitive test performance between the two timepoints. A 2(timepoint: baseline vs. follow-up) by 3(group: HC vs. sPTLD vs. RTH) mixed-design ANOVA was run for each cognitive test that was administered. A main effect of timepoint was observed for the Digit Span test $(F(1, 30) = 4.76, p = .037)$ and Trails A test $(F(1, 29) = 7.50, p = .010)$, with all groups improving on both tests. There also was a main effect of group for the Trails A test $(F(1, 29) = 4.28, p = .024)$. Post-hoc pairwise t-tests for Trails A indicated that the HC group's improvement across visits was marginally significant, $t(15) = -2.04$, $p = .060$). By contrast, the patient groups showed no improvement across visits, (sPTLD: $t(5) = -1.26$, $p = .263$; RTH: $t(9) = -1.53$, $p = .160$). (Supplementary Table 1)

fMRI behavioral task

Mean accuracy and RT (for accurate trials only) were computed for the forward and control tasks at each timepoint. A 2(condition: control vs. forward) x 2(stimulus type: 1 vs. 2) x 3(group: HC vs. sPTLD vs. RTH) mixed-design ANOVA was conducted for the participants' mean accuracy scores at the baseline visit. At baseline, the test yielded a main effect of condition $(F(1, 35) = 8.94, p = .005)$, stimulus type $(F(1, 35) = 26.6, p < .001)$, and an interaction of condition by stimulus type $(F(1, 35) = 7.78, p = .008)$. At follow-up, the ANOVA also yielded a main effect of condition $(F(1, 29) = 6.93, p = .013)$, stimulus type $(F(1, 29) = 20.63, p < .001)$, and an interaction of condition by stimulus type $(F(1, 29) =$

6.00, p = .021). There were no significant effects of group on the mean accuracy at either timepoint. As shown in Fig. 2, the interactions represented the participants' disproportionate difficulty with the two-letters forward condition.

The same 2x2x3 mixed-design ANOVA was conducted for the mean RTs at each timepoint. At the baseline visit, the test yielded a main effect of condition *(F(1, 34) = 40.0, p < .001),* stimulus type *(F(1, 34) = 127.2, p < .001),* and an interaction of condition by stimulus type *(F(1, 34) = 22.7, p < .001).* At 6 months, the ANOVA also yielded a main effect of condition *(F(1, 29) = 20.3, p < .001),* stimulus type *(F(1, 29) = 70.2, p < .001),* and an interaction of condition by stimulus type *(F(1, 29) = 20.8, p < .001).* There were no significant effects of group on the mean RTs at either timepoint. As shown in Fig. 2, as with the accuracy data, RT interactions represented the participants' disproportionate difficulty with the two-letters forward condition. We, therefore, focused our fMRI analyses on this condition.

MRI data

Functional MRI

BOLD signal activations were compared between groups in a double subtraction approach: we obtained within-group contrast values for "two-letters forward" minus "two-letters control" conditions (first subtraction) and then compared these contrast values between groups (second subtraction). Lyme subgroups were collapsed ("All Lyme") and compared to HC, followed by comparisons of each Lyme subgroup to HC and to each other, conducted at both timepoints. Within-group comparisons also were conducted across timepoints.

All Lyme vs. HC

At baseline, between-groups analysis revealed eight activations; all were in the direction of All Lyme participants showing elevated activation compared to HC. (Table 3) Strikingly, six of the eight activations (75%) were located in white matter, located in the frontal lobe, temporal lobe, and cerebellum. With so many areas of activation located in white matter, the observed brain circuitry does not align with prior reports using this fMRI task.[15,31,43] At 6-month follow-up, group differences revealed only two areas of activation, both in the direction of Lyme participants showing greater activation compared to HC, and both located in the frontal lobe (one was in white matter).

RTH vs. HC

At baseline, between-groups analysis yielded 14 activations, all in the direction of RTH showing greater activation compared to HC. Of these, nine (64%) were in white matter. At follow-up, group differences revealed two activations, both in the direction of RTH showing greater activation than HC and located in the frontal lobe (one was in white matter). (Fig. 3) The pattern of activations at both time points closely resembled those observed in the All Lyme vs. HC comparisons, suggesting that the RTH group drove the All Lyme vs. HC results.

sPTLD vs. HC

At baseline, between-groups analysis revealed one gray matter activation in the cerebellum, in the direction of sPTLD showing greater activation compared to HC. At follow-up, group differences revealed one gray matter activation in the frontal lobe, reflecting greater activation in sPTLD compared to HC. (Fig. 3)

RTH vs. sPTLD

At baseline, between-groups analysis revealed two activations, with RTH showing greater activation compared to sPTLD. One activation was located in white matter, and both were in the frontal lobes. At follow-up, group differences revealed one area of greater activation in occipital lobe white matter of RTH compared sPTLD. We expected to see more group differences in the direction of RTH greater than sPTLD, given each subgroup's results compared to HC. Therefore, we explored direct subgroup comparisons using a slightly more liberal threshold of $p < .0025$, $k \leq 10$. Indeed, this revealed four additional activations at baseline, all with the RTH group showing stronger activations than the sPTLD group (three in white matter). At 6 months, five additional activations were revealed in favor of the RTH group showing stronger activations (one in white matter). (Supplementary Fig. 1 and Supplementary Table 2)

Longitudinal Comparisons

Within-group analyses compared activations at baseline and follow-up, but no suprathreshold clusters were revealed.

Tissue class segmentation results

Tissue class segmentation was computed for every ROI. At baseline, 75% of ROIs exceeded 50% white matter for All Lyme vs. HC. However, when RTH vs. HC was examined

separately from sPTLD vs. HC, only the RTH group revealed ROIs that exceeded 50% (64%), thereby driving the All Lyme vs. HC results. RTH vs. sPTLD revealed one ROI (50%) that exceeded 50% white matter. This ROI was located in the frontal lobe and observed in the RTH vs. HC comparison as well. At the 6-month follow-up, there was a reduction in group differences in gray and white matter. The All Lyme vs. HC and RTH vs. HC comparisons were nearly identical, each revealing two ROIs, with one of them exceeding 50% white matter. RTH vs. sPTLD revealed one ROI, which was majority white matter, in the occipital lobe. In summary, white matter ROIs were observed solely in the RTH group, and predominantly at baseline.

Relationship between fMRI and clinical and cognitive scores

ROI values were compared to clinical and cognitive scores at each time point, uncorrected for multiple comparisons, using Spearman's rank correlations. Activation patterns differentiated the two patient groups across time.

For clinical correlates, baseline activation signals from the ROIs in the RTH group generally correlated with better clinical outcomes, regardless of whether the ROIs were found in gray or white matter. (Fig. 4) Thus, increased brain activity was associated with symptomatic improvement. Moreover, white matter activity, despite being highly unusual in fMRI analyses, was consistent with gray matter activity. Six months later, however, this relationship had reversed. ROI activity generally correlated with patients feeling worse. A different pattern was revealed in the sPTLD group. At baseline, ROI activity generally associated with poorer clinical outcomes. Six months later, this relationship had dissipated without a clear association between brain activity and clinical outcomes.

At the baseline visit, correlations between ROI values and cognitive scores did not show clear associations for either group. (Fig. 5) At follow-up, however, the sPTLD group skewed towards negative associations between brain activity and cognitive function, with significant correlates for Digit Symbol Coding (processing speed) and Trails B (executive function). Negative correlates with HVLT Total, Trails A, and FAS COWAT were also quite strong, with $r_s > .6$, which did not meet the threshold using non-parametric testing, but were consistent with difficulties in processing speed, attention, and language functions.

Discussion

This study examined brain changes associated with LD within the first 6 months following antibiotic treatment for acute infection. fMRI baseline activation patterns differed for the RTH and sPTLD groups relative to the HC group, suggesting that the profile of brain activity soon after antibiotic treatment predicts clinical outcomes 6 months later. These quantitative measures following treated *Bb* infection are consistent with our prior report of Lyme-associated brain changes[15] and reflect a biologic mechanism that may underlie patients' reports of neurological symptoms, including brain fog.

The RTH group displayed pervasive and robust gray and white matter activity at baseline relative to that of the HC group. This activity correlated with better self-reported clinical outcomes. Within the SF-36, associations were strongest for non-physical categories, with additional associations with fatigue. Six months later, however, this brain activity had mostly normalized. Only two activations remained, one in gray matter, one in white matter, and both in the frontal lobe. Moreover, brain activity was no longer associated with better clinical outcomes; instead, activity weakly skewed towards worse outcomes. Perhaps, despite a RTH status, prolonged elevated brain activity no longer represented a beneficial response in this group.

A different pattern was observed in the sPTLD group. Overall, there was only one area of gray matter activation at baseline relative to those in HC, located in the cerebellum. The correlations between brain activity and self-reported health variables skewed toward worse clinical outcomes, though these did not reach significance. Six months later, one area of gray matter activation was observed in the left middle frontal gyrus which showed no strong pattern of association with clinical outcomes. Interestingly, brain activation patterns in the sPTLD group at follow-up negatively correlated with cognitive assessments of processing speed, executive function, and attention, which may reflect the subjective experience of brain fog reported by many PTLD patients.

White matter activity during fMRI is unusual due to the decreased energy demands, which are about only about 25% of that of gray matter.[17,44-46] White matter includes myelin and represents axons that interconnect gray matter regions. Synapses are formed in gray matter and most of the energy (delivered by the blood) is needed for brain metabolism there, such as to enable action potentials, restore ion gradients, and release neurotransmitters. Thus, detection of event-related white matter activity via fMRI methods is unconventional.

However, this has been reported elsewhere.[17,18,47] We were struck by the degree to which we observed white matter activity at the baseline measure and that this was exclusive to the RTH group. This activity was mitigated, but not fully resolved, 6 months later. In the sPTLD group, white matter activity was not observed, and gray matter activity overall was less pronounced. Taken together, these findings indicate that white matter activity is an important aspect of the healthy response to *Bb* infection and that early, vigorous white matter activity is a harbinger of a healthy outcome. Our prior findings suggest that people who develop PTLD can also show white matter activity, and this is an indicator of better self-reported clinical outcomes compared to PTLD patients without it.

However, questions remain: what does this white matter activity represent, how is it detected via fMRI, and why does it relate to symptom severity and recovery in LD? Several clues can be gleaned from the data observed here. First, the white matter activity generally correlated with gray matter activity. This indicates that energy metabolism, measured by proxy using the BOLD signal, was required by both brain matter types in synchrony. Second, because axons and myelin in white matter do not have vascularization to support a sufficient BOLD signal, this suggests that the BOLD signal may originate from a source outside of the axon. Third, this phenomenon is not necessarily pathological and may be adaptive because it corresponds to better, not worse, health outcomes.

Any underlying mechanism that could lead to white matter BOLD detection should adhere to these qualities. A promising candidate mechanism may be mediated by astrocytes. This specific type of glial cell has several functions. In white matter, astrocytes assist action potential propagation at the Nodes of Ranvier (NR).[48] Thus, if myelin were damaged or the NR altered, this could lead to increased involvement of astrocytes in white matter in an event-related (i.e., action potential) dependent manner. This would correspond with concurrent astrocytic activity at the synapse in gray matter, where astrocytes use neurovascular coupling to help regulate blood flow needed for energy metabolism in an event-related manner.[49-51] Astrocytic proliferation, known as astrogliosis, is a response to neuronal damage, and this can be helpful or harmful, depending upon the context and duration.[52-55] This attribute fits with the observed elevated activations being beneficial in the early phases for RTH but perhaps less beneficial over a protracted timeframe.

Astrocytic reactivity can be measured in the cerebral spinal fluid (CSF) and blood serum by the protein glial fibrillary acidic protein (GFAP). Although GFAP levels were not obtained in the current study, increased GFAP levels were reported in patients with untreated LD long

ago.[56] Notably, increases were detected within weeks of infection, decreased 4-8 weeks after antibiotic treatment, and correlated with duration of symptoms.[56] This, too, fits with our observed profile of brain activity. Future studies will need to examine the phenomenon of white matter activity in LD more pointedly, including additional measures that target white matter integrity (e.g., diffusion tensor methods), in combination with GFAP and other biomarkers, to better understand how brain activity relates to clinical measures.

These findings may be the direct or indirect result of the initial *Bb* infection. Evidence for spirochetes crossing the blood brain barrier have been elusive, with suggestive evidence from murine models,[57,58] human brain cell cultures,[59] non-human primates,[60] and a human post-mortem study.[61] The effects observed here may, instead, stem from downstream sequelae, such as a systemic inflammatory process following infection, and how the CNS responds to peripheral infection.

Findings from this study should be interpreted with some degree of caution, given the small sample size of the RTH and sPTLD groups. In direct comparison, these subgroups revealed only a few activation differences unless a more liberal threshold was applied. Larger-scale longitudinal studies are needed to confirm these findings. Because the RTH brain imaging results were mitigated, but not entirely resolved, by 6 months, this suggests that participants should be followed longer than 6 months to identify if full resolution occurs.

In summary, this study showed that brain activity alterations occurred soon after treated *Bb* infection, changed over time, and were associated with health outcomes. A major indicator of RTH status was increased brain activity early on and, notably, these occurred mostly in white matter. We postulate the source of white matter activity is related to astrocyte function, but this requires further investigation. Understanding how increased white matter activity is related to RTH in those infected by *Bb* will aid early identification of those most vulnerable to developing PTLD and guide treatment.

Acknowledgements

We thank Jason Creighton, Susan Joseph, and Cheryl Novak for their assistance with recruitment, screening, and data collection.

References

1. Steere AC, Franc S, Wormser GP, et al. Lyme borreliosis. *Nat Rev Dis Primers*. Aug 3 2017;3:17062. doi:10.1038/nrdp.2017.62

2. Marques A. Chronic Lyme disease: a review. *Infect Dis Clin North Am*. Jun 2008;22(2):341-60, vii-viii. doi:10.1016/j.idc.2007.12.011

3. Aucott JN. Posttreatment Lyme disease syndrome. *Infect Dis Clin North Am*. Jun 2015;29(2):309-23. doi:10.1016/j.idc.2015.02.012

4. Wormser GP, Dattwyler RJ, Shapiro ED, et al. The clinical assessment, treatment, and prevention of lyme disease, human granulocytic anaplasmosis, and babesiosis: clinical practice guidelines by the Infectious Diseases Society of America. *Clin Infect Dis*. Nov 1 2006;43(9):1089-134. doi:10.1086/508667

5. Arvikar SL, Crowley JT, Sulka KB, Steere AC. Autoimmune Arthritides, Rheumatoid Arthritis, Psoriatic Arthritis, or Peripheral Spondyloarthritis Following Lyme Disease. *Arthritis Rheumatol*. Jan 2017;69(1):194-202. doi:10.1002/art.39866

6. Rebman AW, Bechtold KT, Yang T, et al. The Clinical, Symptom, and Quality-of-Life Characterization of a Well-Defined Group of Patients with Posttreatment Lyme Disease Syndrome. *Front Med (Lausanne)*. 2017;4:224. doi:10.3389/fmed.2017.00224

7. Rebman AW, Aucott JN. Post-treatment Lyme Disease as a Model for Persistent Symptoms in Lyme Disease. *Front Med (Lausanne)*. 2020;7:57. doi:10.3389/fmed.2020.00057

8. Rebman AW, Aucott JN. Post-treatment Lyme Disease as a Model for Persistent Symptoms in Lyme Disease. *Frontiers in medicine*. 2020;7:57-57. doi:10.3389/fmed.2020.00057

9. Touradji P, Aucott JN, Yang T, Rebman AW, Bechtold KT. Cognitive Decline in Post-treatment Lyme Disease Syndrome. *Arch Clin Neuropsychol*. Jun 1 2019;34(4):455-465. doi:10.1093/arclin/acy051

10. Keilp JG, Corbera K, Slavov I, Taylor MJ, Sackeim HA, Fallon BA. WAIS-III and WMS-III performance in chronic Lyme disease. *J Int Neuropsychol Soc*. Jan 2006;12(1):119-29. doi:10.1017/S1355617706060231

11. Westervelt HJ, McCaffrey RJ. Neuropsychological functioning in chronic Lyme disease. *Neuropsychol Rev*. Sep 2002;12(3):153-77.

12. Coughlin JM, Yang T, Rebman AW, et al. Imaging glial activation in patients with post-treatment Lyme disease symptoms: a pilot study using [(11)C]DPA-713 PET. *J Neuroinflammation*. Dec 19 2018;15(1):346. doi:10.1186/s12974-018-1381-4

13. Fallon BA, Keilp J, Prohovnik I, Heertum RV, Mann JJ. Regional cerebral blood flow and cognitive deficits in chronic lyme disease. *J Neuropsychiatry Clin Neurosci*. Summer 2003;15(3):326-32. doi:10.1176/jnp.15.3.326

14. Newberg A, Hassan A, Alavi A. Cerebral metabolic changes associated with Lyme disease. *Nucl Med Commun*. Aug 2002;23(8):773-7. doi:10.1097/00006231-200208000-00011

15. Marvel CL, Alm KH, Bhattacharya D, et al. A multimodal neuroimaging study of brain abnormalities and clinical correlates in post treatment Lyme disease. *PLoS One*. 2022;17(10):e0271425. doi:10.1371/journal.pone.0271425

16. Gawryluk JR, Mazerolle EL, D'Arcy RC. Does functional MRI detect activation in white matter? A review of emerging evidence, issues, and future directions. *Front Neurosci*. 2014;8:239. doi:10.3389/fnins.2014.00239

17. Gore JC, Li M, Gao Y, et al. Functional MRI and resting state connectivity in white matter - a mini-review. *Magn Reson Imaging*. 2019;63:1-11. doi:10.1016/j.mri.2019.07.017

18. Schilling KG, Li M, Rheault F, et al. Whole-brain, gray, and white matter time-locked functional signal changes with simple tasks and model-free analysis. *Proc Natl Acad Sci U S A*. Oct 17 2023;120(42):e2219666120. doi:10.1073/pnas.2219666120

19. Aucott JN. Slicestudies.org. Accessed 12/11/2024, http://www.slicestudies.org/slice-study-details.html

20. Ware JE, Jr., Sherbourne CD. The MOS 36-item short-form health survey (SF-36). I. Conceptual framework and item selection. *Med Care*. Jun 1992;30(6):473-83.

21. Krupp LB, LaRocca NG, Muir-Nash J, Steinberg AD. The fatigue severity scale. Application to patients with multiple sclerosis and systemic lupus erythematosus. *Arch Neurol*. Oct 1989;46(10):1121-3. doi:10.1001/archneur.1989.00520460115022

22. Dworkin RH, Turk DC, Revicki DA, et al. Development and initial validation of an expanded and revised version of the Short-form McGill Pain Questionnaire (SF-MPQ-2). *Pain*. Jul 2009;144(1-2):35-42. doi:10.1016/j.pain.2009.02.007

23. Beck A, Steer R, Brown G. *Beck Depression Inventory*. 2nd ed. The Psychological Corporation; 1996.

24. Aucott JN, Yang T, Yoon I, Powell D, Geller SA, Rebman AW. Risk of post-treatment Lyme disease in patients with ideally-treated early Lyme disease: A prospective cohort study. *Int J Infect Dis*. Mar 2022;116:230-237. doi:10.1016/j.ijid.2022.01.033

25. Aucott JN, Crowder LA, Kortte KB. Development of a foundation for a case definition of post-treatment Lyme disease syndrome. *Int J Infect Dis*. Jun 2013;17(6):e443-9. doi:10.1016/j.ijid.2013.01.008

26. Wilkinson GS, Robertson GJ. Wide Range Achievement Test 4 Professional manual. *Lutz, FL: Psychological Assessment Resources*. 2006;48

27. Wechsler D. *Weschler Adult Intelligence Scale*. San Antonio, TX: Pearson Assessment 2008.

28. Benedict RH, Schretlen D, Groninger L, Brandt J. Hopkins Verbal Learning Test–Revised: Normative data and analysis of inter-form and test-retest reliability. *The Clinical Neuropsychologist*. 1998;12(1):43-55.

29. Office AGs. *Army Individual Test Battery: Manual of directions and scoring*. War Department; 1944.

30. Benton AL, Sivan, A.B., Hamsher, K. Varney, N.R., and Spreen, O. . *Contributions to neuropsychological assessment* 2nd ed. Oxford University Press, USA; 1994.

31. Marvel CL, Desmond JE. From storage to manipulation: How the neural correlates of verbal working memory reflect varying demands on inner speech. *Brain Lang*. Jan 2012;120(1):42-51. doi:10.1016/j.bandl.2011.08.005

32. Marvel CL, Faulkner ML, Strain EC, Mintzer MZ, Desmond JE. An fMRI investigation of cerebellar function during verbal working memory in methadone maintenance patients. Research Support, N.I.H., Extramural

Research Support, Non-U.S. Gov't. *Cerebellum*. Mar 2012;11(1):300-10. doi:10.1007/s12311-011-0311-0

33. Berenbaum JG, Nadkarni PA, Marvel CL. An fMRI analysis of verbal and non-verbal working memory in people with a past history of opioid dependence. Original Research. *Frontiers in Neuroscience*. 2023-April-05 2023;17doi:10.3389/fnins.2023.1053500

34. Chen SHA, Desmond JE. Temporal dynamics of cerebro-cerebellar network recruitment during a cognitive task. *Neuropsychologia*. 2005/01/01/ 2005;43(9):1227-1237. doi:https://doi.org/10.1016/j.neuropsychologia.2004.12.015

35. Marvel CL, Desmond JE. From storage to manipulation: How the neural correlates of verbal working memory reflect varying demands on inner speech. *Brain and Language*. 2012/01/01/ 2012;120(1):42-51. doi:https://doi.org/10.1016/j.bandl.2011.08.005

36. B M, JL A, R V, JB P. Region of interest analysis using an SPM toolbox [abstract] Presented at the , June 2-6, 2002, . Available on CD-ROM in presented at: 8th International Conference on Functional Mapping of the Human Brain; 2002; Sendai, Japan.

37. Talairach J, Tournoux P. *Co-planar Stereotaxic atlas of the human brain 3-D proportional system, An approach to cerebral imaging*. M R. Thieme Medical Publishers, Inc.; 1988.

38. Schmahmann JD, Doyen J, Toga AW, Petrides M, Evans AC. *MRI Atlas of the Human Cerebellum*. Academic Press; 2000.

39. Klein A, Andersson J, Ardekani BA, et al. Evaluation of 14 nonlinear deformation algorithms applied to human brain MRI registration. *Neuroimage*. 2009;46(3):786-802. doi:10.1016/j.neuroimage.2008.12.037

40. Yushkevich PA, Avants BB, Pluta J, et al. A high-resolution computational atlas of the human hippocampus from postmortem magnetic resonance imaging at 9.4 T. *Neuroimage*. 2009;44(2):385-398. doi:10.1016/j.neuroimage.2008.08.042

41. Zhang Y, Brady M, Smith S. Segmentation of brain MR images through a hidden Markov random field model and the expectation-maximization algorithm. *IEEE Transactions on Medical Imaging*. 2001;20(1):45-57. doi:10.1109/42.906424

42. Eggert LD, Sommer J, Jansen A, Kircher T, Konrad C. Accuracy and Reliability of Automated Gray Matter Segmentation Pathways on Real and Simulated Structural Magnetic Resonance Images of the Human Brain. *PLOS ONE*. 2012;7(9):e45081. doi:10.1371/journal.pone.0045081

43. Chen SH, Desmond JE. Temporal dynamics of cerebro-cerebellar network recruitment during a cognitive task. *Neuropsychologia*. 2005;43(9):1227-37. doi:10.1016/j.neuropsychologia.2004.12.015

44. Logothetis NK. The underpinnings of the BOLD functional magnetic resonance imaging signal. *J Neurosci*. May 15 2003;23(10):3963-71.

45. Rostrup E, Law I, Blinkenberg M, et al. Regional Differences in the CBF and BOLD Responses to Hypercapnia: A Combined PET and fMRI Study. *Neuroimage*. 2000/02/01/ 2000;11(2):87-97. doi:10.1006/nimg.1999.0526

46. Harris JJ, Attwell D. The Energetics of CNS White Matter. *The Journal of Neuroscience*. 2012;32(1):356. doi:10.1523/JNEUROSCI.3430-11.2012

47. Gawryluk JR, Mazerolle EL, D'Arcy RCN. Does functional MRI detect activation in white matter? A review of emerging evidence, issues, and future directions. *Frontiers in neuroscience*. 2014;8:239-239. doi:10.3389/fnins.2014.00239

48. Butt AM, Verkhratsky A. Astrocytes regulate action potential propagation in myelinated axons: It is very crowded at the node of Ranvier. *Cell Calcium*. Jan 2022;101:102518. doi:10.1016/j.ceca.2021.102518

49. Howarth C, Mishra A, Hall CN. More than just summed neuronal activity: how multiple cell types shape the BOLD response. *Philos Trans R Soc Lond B Biol Sci*. Jan 4 2021;376(1815):20190630. doi:10.1098/rstb.2019.0630

50. Howarth C. The contribution of astrocytes to the regulation of cerebral blood flow. *Front Neurosci*. 2014;8:103. doi:10.3389/fnins.2014.00103

51. Lia A, Di Spiezio A, Speggiorin M, Zonta M. Two decades of astrocytes in neurovascular coupling. *Front Netw Physiol*. 2023;3:1162757. doi:10.3389/fnetp.2023.1162757

52. Liddelow SA, Olsen ML, Sofroniew MV. Reactive Astrocytes and Emerging Roles in Central Nervous System (CNS) Disorders. *Cold Spring Harb Perspect Biol*. Jul 1 2024;16(7)doi:10.1101/cshperspect.a041356

53. Sofroniew MV. Astrocyte barriers to neurotoxic inflammation. *Nat Rev Neurosci*. May 2015;16(5):249-63. doi:10.1038/nrn3898

54. Jang E, Kim JH, Lee S, et al. Phenotypic polarization of activated astrocytes: the critical role of lipocalin-2 in the classical inflammatory activation of astrocytes. *J Immunol*. Nov 15 2013;191(10):5204-19. doi:10.4049/jimmunol.1301637

55. Liddelow SA, Guttenplan KA, Clarke LE, et al. Neurotoxic reactive astrocytes are induced by activated microglia. *Nature*. Jan 26 2017;541(7638):481-487. doi:10.1038/nature21029

56. Dotevall L, Rosengren LE, Hagberg L. Increased cerebrospinal fluid levels of glial fibrillary acidic protein (GFAp) in Lyme neuroborreliosis. *Infection*. Mar-Apr 1996;24(2):125-9. doi:10.1007/BF01713316

57. Casselli T, Divan A, Vomhof-DeKrey EE, Tourand Y, Pecoraro HL, Brissette CA. A murine model of Lyme disease demonstrates that Borrelia burgdorferi colonizes the dura mater and induces inflammation in the central nervous system. *PLoS Pathog*. Feb 2021;17(2):e1009256. doi:10.1371/journal.ppat.1009256

58. Divan A, Casselli T, Narayanan SA, et al. Borrelia burgdorferi adhere to blood vessels in the dura mater and are associated with increased meningeal T cells during murine disseminated borreliosis. *PLoS One*. 2018;13(5):e0196893. doi:10.1371/journal.pone.0196893

59. Grab DJ, Perides G, Dumler JS, et al. Borrelia burgdorferi, host-derived proteases, and the blood-brain barrier. *Infect Immun*. Feb 2005;73(2):1014-22. doi:10.1128/IAI.73.2.1014-1022.2005

60. Crossland NA, Alvarez X, Embers ME. Late Disseminated Lyme Disease: Associated Pathology and Spirochete Persistence Posttreatment in Rhesus Macaques. *Am J Pathol*. Mar 2018;188(3):672-682. doi:10.1016/j.ajpath.2017.11.005

61. Gadila SKG, Rosoklija G, Dwork AJ, Fallon BA, Embers ME. Detecting Borrelia Spirochetes: A Case Study With Validation Among Autopsy Specimens. *Front Neurol*. 2021;12:628045. doi:10.3389/fneur.2021.628045

Fig. legends

Fig. 1 Study recruitment and retention data. Description of sample sizes for both study groups from consent to completion.

Fig. 2 Boxplots comparing accuracy and response times on the working memory task across groups. Results are shown for the "two-letters forward" condition, which was the most challenging condition that was used for the fMRI data analysis. Data represent each group at baseline *(left)* and 6-month follow-up *(right)* time points for accuracy (*top*) and response time (*bottom*) measures. Boxes represent the interquartile range, with the median denoted by the horizontal line within. Whiskers extend to 10^{th} and 90^{th} percentiles, and points beyond are considered outliers. Groups did not significantly differ. See Supplementary Table 1 for complete fMRI task results.

Fig. 3 fMRI cluster overlays representing between-group activation differences during baseline and follow-up scans. A) RTH > HC: Numerous activation differences were evident at baseline (red-yellow), but only two activation differences remain 6 months later (blue). **B)** sPTLD > HC: Few activation differences at baseline or follow-up were observed. Cross-reference with Table 3 for cluster information. Scale shows t-values 0 – 6. Images shown in neurological convention with right side on the right. Threshold = $p < .001$ and $k \geq 10$.

Fig. 4 Correlation matrix for ROI values and clinical assessment scores. Shades of red = positive correlation direction; shades of blue = negative correlation direction. Note that the SF-36 uses an inverse relationship to severity of illness. Correlations were run using Spearman's rank; significance is denoted by * <.05 if correlations also passed visual scatterplot inspection.

Fig. 5 Correlation matrix for ROI values and cognitive test scores. Shades of red = positive correlation direction; shades of blue = negative correlation direction. Note that the SF-36 uses an inverse relationship to severity of illness Correlations were run using Spearman's rank; significance is denoted by * <.05, ** < .01 if correlations also passed visual scatterplot inspection.

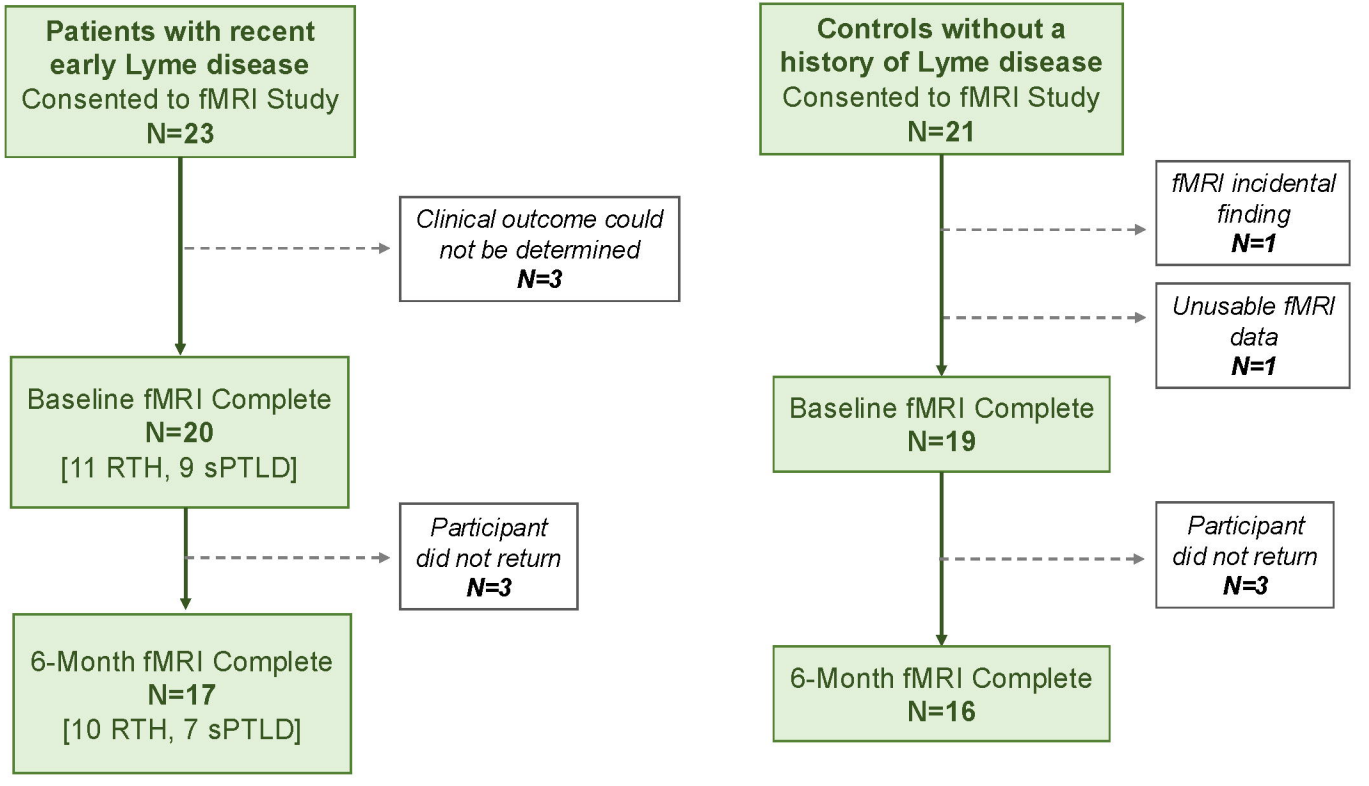
Patients with recent early Lyme disease
Consented to fMRI Study
N=23
Clinical outcome could not be determined
N=3
Baseline fMRI Complete
N=20
[11 RTH, 9 sPTLD]
Participant did not return
N=3
6-Month fMRI Complete
N=17
[10 RTH, 7 sPTLD]
Controls without a history of Lyme disease
Consented to fMRI Study
N=21
fMRI incidental finding
N=1
Unusable fMRI data
N=1
Baseline fMRI Complete
N=19
Participant did not return
N=3
6-Month fMRI Complete
N=16

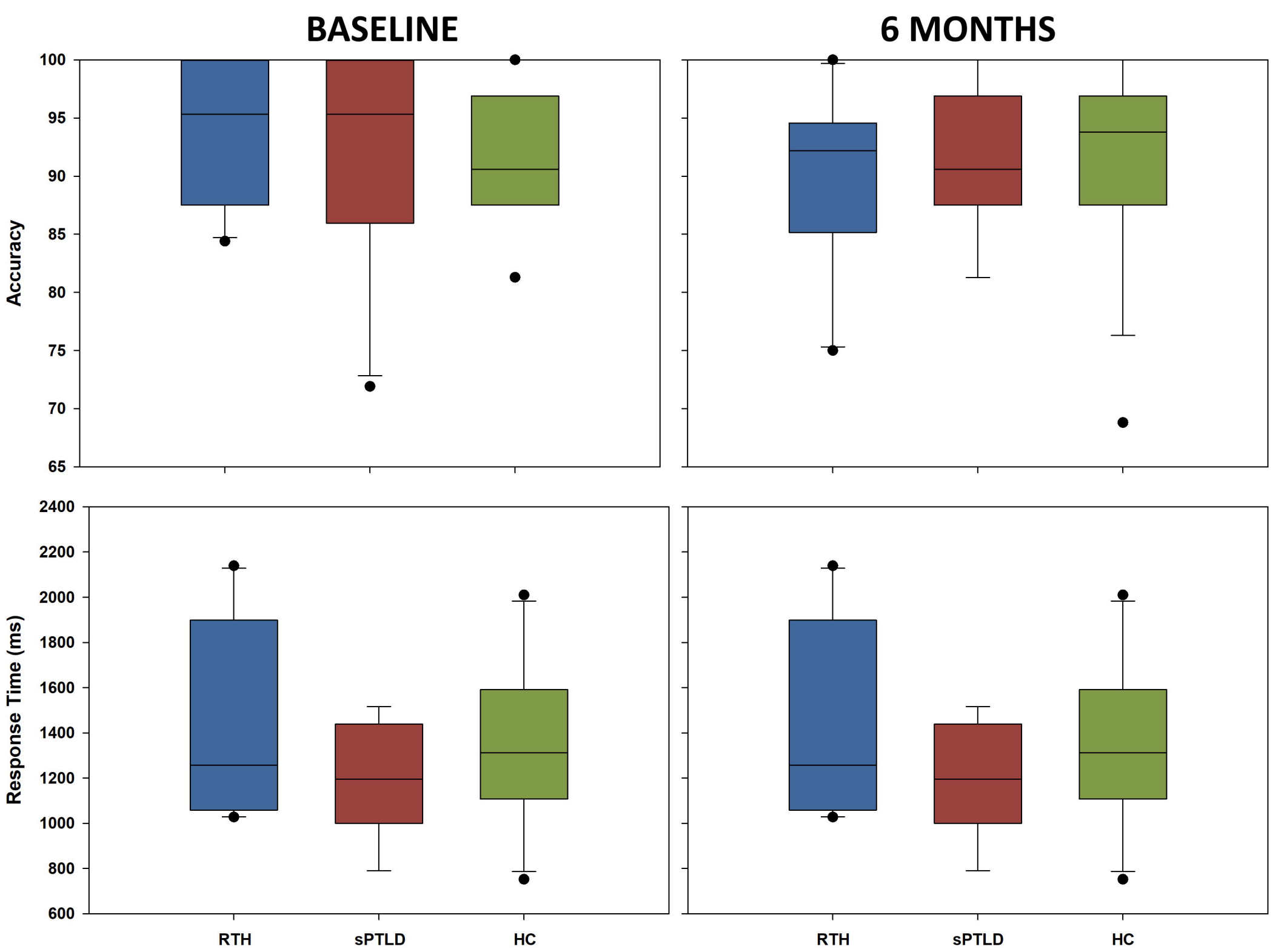
BASELINE
6 MONTHS
Accuracy
100
95
90
85
80
75
70
65
Response Time (ms)
2400
2200
2000
1800
1600
1400
1200
1000
800
600
RTH
sPTLD
HC
RTH
sPTLD
HC

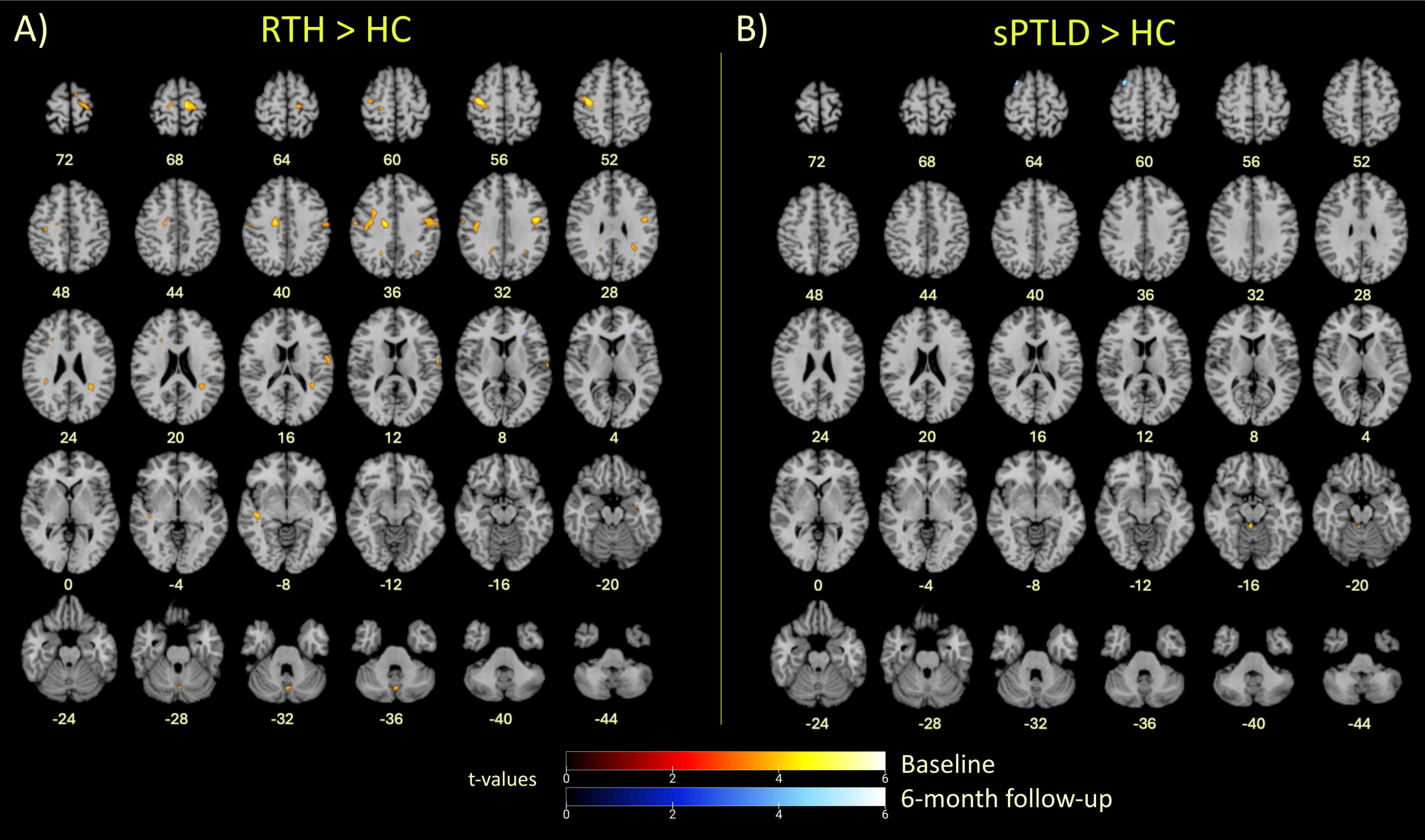
A)
RTH > HC
B)
sPTLD > HC
72
68
64
60
56
52
48
44
40
36
32
28
24
20
16
12
8
4
0
-4
-8
-12
-16
-20
-24
-28
-32
-36
-40
-44
t-values
0
2
4
6
Baseline
6-month follow-up

		Regions of Activation	Health Surveys												
			SF-36									PLQS Total Number	BDI Total Score	Fatigue Severity Scale Total	McGill Pain Total Score
			Mental Component	Mental Health	Role Emotional	Social Function	Vitality	General Health	Bodily Pain	Role Physical	Physical Function	Physical Component				
			Baseline Visit												
RTH > HC	WM	*L Frontal Lobe (-16, -12, 38)*	0.673	0.280	0.250	**0.657***	**0.618***	0.378	0.381	0.380	0.175	0.173	**-0.655***	0.432	**-0.663***	-0.489
		L Parietal Lobe (-22, -56, 36)	-0.173	-0.187	0.615	0.311	0.249	**0.633***	0.237	0.472	0.569	**0.664***	-0.201	-0.178	0.000	0.127
		L Frontal Lobe (-24, 22, 20)	0.600	0.439	0.708	**0.708***	0.548	0.469	0.353	0.167	0.450	0.364	-0.445	0.322	-0.401	-0.693
		L Frontal Lobe (-30, 4, 36)	0.273	-0.150	0.400	0.454	0.433	0.551	0.274	0.500	0.238	0.336	-0.347	0.110	-0.571	-0.114
		L Frontal Lobe (-34, -18, 54)	0.173	-0.154	0.325	0.392	0.396	**0.624***	0.255	0.352	0.288	0.336	-0.215	0.226	-0.602	0.102
		L Parietal Lobe (-34, -36, 26)	0.291	0.173	0.708	**0.612***	0.530	**0.738***	0.487	0.380	0.663	0.673	-0.401	0.034	-0.231	-0.369
		L Temporal Lobe (-42, -22, -8)	0.573	0.229	0.383	**0.749***	0.461	0.164	0.111	0.259	-0.019	-0.009	-0.523	0.432	-0.456	-0.089
		L Frontal Lobe (-8, -20, 70)	0.273	-0.159	0.209	0.418	0.318	0.478	0.060	0.426	-0.088	0.073	-0.391	0.350	**-0.711***	0.369
		L Parietal Lobe (30, -44, 24)	0.136	-0.182	0.574	0.591	0.277	0.246	0.274	0.259	0.244	0.373	-0.303	-0.089	-0.134	-0.280
	GM	*R Superior Frontal Gyrus (BA 6) (12, -22, 68)*	0.373	-0.042	0.342	**0.652***	0.415	0.337	0.149	0.435	-0.006	0.100	-0.347	0.219	-0.450	0.273
		R Cerebellar Vernis VIIB (2, -72, 32)	0.109	0.075	0.749	0.494	0.189	0.355	0.060	0.148	0.306	0.373	-0.367	0.171	-0.122	-0.127
		R Hippocampus (36, -10, -20)	0.336	0.196	0.540	**0.627***	0.507	0.442	0.232	0.278	0.444	0.373	-0.567	0.452	-0.419	-0.248
		R Precentral Gyrus (BA 6) (46, -9, 32)	0.191	-0.070	0.592	0.357	0.267	**0.610***	0.079	0.352	0.206	0.327	-0.357	0.199	-0.584	-0.044
		R Postcentral Gyrus (BA 43) (62, -8, 12)	0.573	0.369	0.650	0.612	0.475	0.538	0.158	0.306	0.244	0.255	**-0.621***	0.452	-0.614	-0.375
sPTLD > HC	GM	*L Cerebellar Lobule III (4, -40, -18)*	-0.429	-0.293	-0.575	-0.386	-0.422	-0.168	-0.096	-0.371	-0.675	-0.405	0.374	0.050	0.168	*0.712**
			6 Month Follow-Up Visit												
RTH > HC	WM	*R Frontal Lobe (34, 32, 6)*	0.345	0.274	0.000	-0.174	-0.551	-0.412	-0.206	-0.206	-0.559	*-0.648**	0.266	-0.020	0.042	0.610
	GM	*L Middle Frontal Gyrus (BA 6) (-28, 10, 58)*	0.152	0.247	-0.435	-0.522	-0.506	-0.326	-0.295	-0.308	-0.445	-0.442	-0.266	-0.269	0.515	**0.662***
sPTLD > HC	GM	*L Middle Frontal Gyrus (BA 6) (-30, 10, 62)*	0.000	0.180	-0.079	0.424	0.164	-0.468	0.505	0.482	0.265	0.714	0.270	-0.357	0.432	0.000

		Regions of Activation	Cognitive Tasks										
			WRAT	Digit Span	Coding	HVLT Total	HVLT Delayed	Trails A	Trails B	fMRI Accuracy	fMRI Reaction Time	FAS COWAT	Animals COWAT
			Baseline Visit										
RTH > HC	WM	*L Frontal Lobe (-16, -12, 38)*	-0.338	-0.149	-0.204	**0.680***	0.253	-0.255	-0.037	-0.195	-0.309	-0.317	-0.212
		L Parietal Lobe (-22, -56, 36)	0.174	-0.009	0.370	-0.251	-0.248	0.005	-0.266	0.157	0.127	-0.305	0.067
		L Frontal Lobe (-24, 22, 20)	-0.119	-0.265	-0.324	0.247	-0.175	-0.588	-0.248	-0.271	0.006	-0.274	0.139
		L Frontal Lobe (-30, 4, 36)	-0.132	0.074	0.398	0.434	0.382	-0.018	0.009	0.245	-0.418	-0.091	0.055
		L Frontal Lobe (-34, -18, 54)	0.100	0.293	0.185	0.219	0.074	-0.105	0.018	0.183	-0.321	0.006	0.261
		L Parietal Lobe (-34, -36, 26)	0.169	-0.060	0.083	-0.041	-0.271	-0.469	-0.229	-0.220	0.152	-0.122	0.297
		L Temporal Lobe (-42, -22, -8)	-0.187	-0.070	-0.296	0.347	-0.244	-0.087	-0.193	0.000	-0.079	-0.213	0.042
		L Frontal Lobe (-8, -20, 70)	-0.055	0.261	0.343	0.361	0.166	0.114	0.156	0.138	-0.539	-0.079	-0.006
		L Parietal Lobe (30, -44, 24)	0.315	0.167	0.259	0.256	0.074	-0.219	-0.046	0.013	0.188	0.091	0.479
	GM	*R Superior Frontal Gyrus (BA 6) (12, -22, 68)*	-0.064	0.158	0.102	0.201	-0.202	0.100	-0.092	0.239	-0.212	0.012	0.212
		R Cerebellar Vernis VIIB (2, -72, 32)	0.224	-0.093	0.074	-0.073	-0.303	-0.292	-0.202	-0.151	0.200	-0.317	0.176
		R Hippocampus (36, -10, -20)	-0.014	-0.140	-0.269	0.119	-0.317	-0.219	-0.385	-0.145	0.248	-0.409	-0.030
		R Precentral Gyrus (BA 6) (46, -9, 32)	-0.023	0.005	0.472	0.237	0.253	-0.150	0.046	0.025	-0.382	-0.171	0.030
		R Postcentral Gyrus (BA 43) (62, -8, 12)	-0.260	-0.312	-0.009	0.292	-0.023	-0.351	-0.147	-0.290	-0.224	-0.451	-0.236
sPTLD > HC	GM	*L Cerebellar Lobule III (4, -40, -18)*	0.467	0.605	0.210	0.109	0.385	0.787	0.433	0.026	0.067	0.071	0.071
			6 Month Follow-Up Visit										
RTH > HC	WM	*R Frontal Lobe (34, 32, 6)*	n/a	0.190	-0.235	0.269	0.288	0.140	0.220	0.474	0.406	0.067	0.321
	GM	*L Middle Frontal Gyrus (BA 6) (-28, 10, 58)*	n/a	0.550	0.154	0.061	-0.092	-0.152	0.128	**0.862****	0.345	0.400	0.429
sPTLD > HC	GM	*L Middle Frontal Gyrus (BA 6) (-30, 10, 62)*	n/a	-0.273	**-0.891****	-0.750	-0.582	-0.638	**-0.893****	-0.037	0.393	-0.657	-0.486

Table 1 Baseline demographic and clinical characteristics

	RTH (*n*=11)	**sPTLD (*n*=9)**	**HC (*n*=19)**
Age (years)	56.51 (14.57)	47.14 (14.72)	51.16 [37.47, 57.93]
Male Gender	5 (45.45%)	6 (66.67%)	6 (31.58%)
Education (Years)	16.55 (2.62)	16.78 (2.22)	16.53 (1.98)
Two-Tier Seropositive[1]	5/10[1] (50.00%)	6 (66.67%)	0 (0.00%)
Disseminated EM Lesions[2]	6 (54.44%)	3 (33.33%)	N/A
Lyme Disease Duration Prior to Treatment (Days)	6.59 (4.85)	6.00 [3.00, 6.00]	N/A
Lyme Disease Duration at first fMRI (Days)	36.00 [31.00, 52.00]	40.89 (8.49)	N/A
Days Since Stopping Doxycycline at First Scan (Days)[3]	10.00 [4.00, 26.00]	13.0 (4.97)	N/A
Days Between MRI Scans[4]	192.00 (18.28), n=10	199.14 (23.57), n=7	184.50 [179.50, 201.50], n=16

N (%) are presented for categorical variables. Mean (standard deviation) are presented for normally distributed continuous variables, and median [IQR] are presented for non-normally distributed continuous variables. Sample sizes are presented when missing data occurred. No group differences were found across variables, all p-values > .214.

[1]Based on acute and convalescent testing interpreted according to CDC criteria which account for illness duration at the time of the test. One RTH patient was missing complete serostatus information.

[2]No patients had early disseminated neurologic or cardiac Lyme disease at the time of diagnosis.

[3]One person was at the end of their doxycycline treatment when the first scan was performed.

[4] One RTH, two sPTLD, and three HC participants did not return for their 6-month MRI scan.

Table 2 Standardized symptom measures

	Baseline Visit		6-Month Follow-up	
	RTH	sPTLD	RTH	sPTLD
	n=11	*n*=9	*n*=10	*n*=7
Beck Depression Inventory-II Total	4.82 (3.76)	9.43 (7.91), n=7	.00 [.00, 3.00], n=9*	6.57 (6.58)*
Beck Depression Inventory-II Cognitive/Affective Subscale	1.00 [.00, 3.00]	4.29 (3.90), n=7	.00 [.00, 0.00], n=9*	4.00 (5.00)*
Beck Depression Inventory-II Somatic Subscale	2.82 (1.83)	5.14 (4.41), n=7	.00 [.00, 1.00], n=9	2.57 (2.07)
SF-36 Mental Health	57.95 (4.33)	46.84 (14.16), n=8	58.46 [55.64, 58.46]	52.83 (9.34)
SF-36 Role Emotional	55.88 [51.99, 55.88]	53.94 [32.56, 55.88], n=8	55.88 [55.88, 55.88]	55.88 [36.44, 55.88]
SF-36 Social Functioning	56.85 [45.94, 56.85]*	37.76 (15.97), n=8*	56.85 [56.85, 56.85]	45.94 [45.94, 56.85]
SF-36 Vitality	51.24 (9.78)	42.33 (15.87), n=8	58.33 [58.33, 61.46]	52.09 (11.40)
SF-36 General Health	53.00 (8.73)	51.03 (7.81), n=8	57.23, [55.32, 62.47]	52.46 (6.34)
SF-36 Bodily Pain	52.17 (8.12)	43.68 (15.33), n=8	55.36 [55.36, 55.36]	53.49 (8.61)
SF-36 Role Physical	49.28 (6.97)	40.63 (15.54), n=8	56.85 [54.40, 56.85]	50.55 (7.46)
SF-36 Physical Functioning	51.77 [42.30, 57.03]	52.82 [43.55, 55.98], n=8	54.93 [50.72, 57.03]	54.93 [50.72, 57.03]
SF-36 Mental Component	56.87 (5.41)*	42.60 (15.44), n=8*	56.90 [56.10, 58.19]	49.69 (10.84)
SF-36 Physical Component	47.80 (9.25)	46.37 (11.02), n=8	56.16 [55.08, 57.48]	53.30 (3.35)
Post-Lyme Questionnaire of Symptoms Total	1.00 [.00, 1.00]*	3.00 [1.00, 5.50], n=8*	.00 [.00, 1.00]*	2.00 [1.00, 6.00]*
Post-Lyme Questionnaire of Symptoms Cognitive Subscale	0.00 (0.00)	.00 [.00, 1.00], n=8	.00 [.00, 1.00]	.00 [.00, .00]
Post-Lyme Questionnaire of Symptoms Neuro Subscale	.00 [.00, 1.00]	1.75 (2.05), n=8	.00 [.00, .00]	1.00 [.00, 2.00]
Fatigue Severity Scale Total	23.80 (12.44), n=10	34.13 (21.82), n=8	19.30 (9.37)	22.71 (12.87)
Short Form McGill Pain Questionnaire Total	1.00 [.00, 2.00], n=10	3.38 (4.17), n=8	0.50 [.00, 2.00]	3.57 (4.43)
Short Form McGill Pain Questionnaire Affective Subscale	.00 [.00, 1.00], n=10	.00 [.00, 1.50], n=8	.00 [.00, .00]	0.00 [0.00, 0.00]
Short Form McGill Pain Questionnaire Sensory Subscale	.50 [.00, 1.00], n=10	2.63 (3.29), n=8	0.50 [.00, 2.00]	3.43 (4.12)

Mean (standard deviation) are presented for normally distributed continuous variables, and median [IQR] are presented for non-normally distributed continuous variables.
Sample n's are presented for any measures with missing data.
Significant group differences are marked for each test '*' = sPTLD vs. RTH, $p < .05$.

Table 3 FMRI activation differences during the fMRI working memory task at baseline and 6-month follow-up.

Cluster size (voxels)	T-value	X, Y, Z (MNI)	Brain Region (BA)	% White Matter
Baseline Regions of Activation				
			All Lyme > HC	
67	4.31	-42, -22, -8	L Temporal Lobe	**91***
36	4.25	-16, -12, 36	L Frontal Lobe	**100**
65	4.04	-36, -16, 54	L Frontal Lobe	**56***
54	4.03	12, -22, 68	R Frontal superior gyrus (BA 6)	47*
26	3.83	-32, 4, 36	L Frontal Lobe	**95**
31	3.68	-16, -48, -28	L Cerebellar Anterior Lobe	**97**
11	3.66	-50, 18, 18	L Frontal Lobe	**61**
21	3.58	2, -72, -36	R Cerebellar Vermis VIIB	9
			HC > All Lyme	
None				
			RTH > HC	
134	5.45	-16, -12, 38	L Frontal Lobe	**97***
217	5.01	-34, -18, 54	L Frontal Lobe	**52***
190	4.77	12, -22, 68	R Superior frontal gyrus (BA 6)	41*
191	4.60	46, -8, 32	R Precentral Gyrus (BA 6)	41*
63	4.33	-42, -22, -8	L Temporal Lobe	**87***
198	4.19	-30, 4, 36	L Frontal Lobe	**78***
152	4.00	30, -44, 24	R Parietal Lobe	**99***
64	3.98	2, -72, -32	R Cerebellar Vermis VIIB	12*
26	3.97	-8, -20, 70	L Frontal Lobe	**84**
81	3.94	62, -8, 12	R Postcentral Gyrus (BA 43)	32*
32	3.92	-22, -56, 36	L Parietal Lobe	**100**
15	3.81	-24, 22, 20	L Frontal Lobe	**100**
10	3.78	36, -10, -20	R Hippocampus	20
26	3.77	-34, -36, 26	L Parietal Lobe	**99**
			HC > RTH	
None				
			sPTLD > HC	
25	4.37	-4, -40, -18	L Cerebellar Lobule III	29
			HC > sPTLD	
None				
			RTH > sPTLD	
78	4.13	48, -10, 32	R Post Central Gyrus (BA 4)	9*
10	3.93	-18, -12, 40	L Frontal Lobe	**100**
			sPTLD > RTH	
None				
6 Month Follow-up Regions of Activation				
			All Lyme > HC	

32	4.38	-28, 10, 60	L Middle Frontal Gyrus (BA 6)	4
10	4.02	34, 34, 6	R Frontal Lobe	**96**
			HC > All Lyme	
None				
			RTH > HC	
17	4.60	34, 32, 6	R Frontal Lobe	**78**
10	3.86	-28, 10, 58	L Middle Frontal Gyrus (BA 6)	1
			HC > RTH	
None				
			sPTLD > HC	
50	5.81	-30, 10, 62	L Middle Frontal Gyrus (BA 6)	8
			HC > sPTLD	
None				
			RTH > sPTLD	
15	4.57	42, -80, 18	R Occipital Lobe	**56**
			sPTLD > RTH	
13	4.34	-56, 20, 14	L Inferior Frontal Gyrus (BA 45)	0
17	4.30	58, 20, 20	R Inferior Frontal Gyrus (BA 45)	15

Threshold = $p < .001$ and $k \geq 10$. MNI = Montreal Neurological Institute coordinates;
BA = Brodmann Area.
For white matter > 50%, the brain region was reported within the relevant lobe rather than the BA.
Bold % white matter indicates > 50%.
* indicates the activation passed $p < .001$ and also surpassed $k \geq$ expected voxels per cluster (i.e., beyond $k \geq 10$ voxels